A Computational Study on the Kinetics and Mechanism for the Unimolecular Decomposition of *o*-Nitrotoluene

S. C. Chen,[†] S. C. Xu,[‡] E. Diau,[†] and M. C. Lin*[,‡]

Department of Applied Chemistry, Institute of Molecular Science, National Chiao Tung University, Hsichu, Taiwan 300, and Department of Chemistry, Emory University, Atlanta, Georgia 30322

Received: April 17, 2006; In Final Form: June 23, 2006

The kinetics and mechanism for the unimolecular decomposition of *o*-nitrotoluene (*o*-$CH_3C_6H_4NO_2$) have been studied computationally at the G2M(RCC, MP2)//B3LYP/6-311G(d, p) level of theory in conjunction with rate constant predictions with RRKM and TST calculations. The results of the calculations reveal 10 decomposition channels for *o*-nitrotoluene and its six isomeric intermediates, among them four channels give major products: $CH_3C_6H_4 + NO_2$, $C_6H_4C(H)ON$ (anthranil) + H_2O, $CH_3C_6H_4O$ (*o*-methyl phenoxy) + NO, and $C_6H_4C(H_2)NO$ + OH. The predicted rate constants in the 500−2000 K temperature range indicate that anthranil production, taking place initially by intramolecular H-abstraction from the CH_3 group by NO_2 followed by five-membered ring formation and dehydration, dominates at temperatures below 1000 K, whereas NO_2 elimination becomes predominant above 1100 K and $CH_3C_6H_4O$ formation by the nitro−nitrite isomerization/decomposition process accounts for only 5−11% of the total product yield in the middle temperature range 800−1300 K. The branching ratio for $CH_2C_6H_4NO$ formation by the decomposition process of $CH_2C_6H_4N(O)OH$ is negligible. The predicted high-pressure-limit rate constants with the rate expression of 4.10×10^{17} exp[−37000/*T*] s^{-1} for the NO_2 elimination channel and 9.09×10^{12} exp[−25800/*T*] s^{-1} for the H_2O elimination channel generally agree reasonably with available experimental data. The predicted high-pressure-limit rate constants for the NO and OH elimination channels are represented as 1.49×10^{14} exp[−30000/*T*] and 1.31×10^{15} exp[−38000/*T*] s^{-1}, respectively.

Introduction

The thermal decomposition of *o*-nitrotoluene (1-nitro, 2-methyl benzene) has received much attention thanks to its relevance to the trinitrotoluene decomposition chemistry. Gonzalez and co-workers[1] studied the kinetics of the decomposition reaction in an experiment by high-power infrared laser heating (laser-enhanced homogeneous pyrolysis). In the experiment, they used a Lumonics K103 CO_2 laser (wavelength = 10.6 μm, duration = 1 μs, fluence = 1 J/cm^2) at a constant repetition rate (0.2 Hz) for the irradiation of a small portion of the reaction cell (typically 24%). They reported that the primary decomposition process occurred by the breaking of the C−NO_2 bond with 70.2 ± 2.5 kcal/mol activation energy at 1100 K. The rate expression for the dissociation process *o*-$CH_3C_6H_4NO_2 \rightarrow CH_3C_6H_4 + NO_2$ at 110 Torr SF_6 pressure over the temperature range 1110−1250 K was given by $k_1 = 10^{15.9}\pm0.5$ exp[−(33000 ± 1000)/*T*] s^{-1}. Tsang and co-workers[2,3] also studied the decomposition reaction in a single-pulse shock tube at 2700−3400 Torr Ar pressure over the temperature range 1000−1180 K. They obtained the rate expressions of $k_1 = 6.4 \times 10^{14}$ exp[−30900/*T*] s^{-1} for NO_2 production and $k_2 = 1.2 \times 10^{13}$ exp[−26000/*T*] s^{-1} for *o*-$CH_3C_6H_4NO_2 \rightarrow C_6H_4C(H)ON$ (anthranil) + H_2O, respectively.

The photodissociation of nitrotoluene has been studied using a femtosecond laser photolysis/mass spectroscopic technique at 375 nm.[4] Both NO_2 and NO loss channels have been observed for all three nitrotoluene isomers (*o*-, *m*- and *p*-nitrotoluenes). In the dissociation of *o*-nitrotoluene, OH is a significant product that can be attributed to the so-called "ortho effect" (i.e., H-transfer from the CH_3- to the NO_2-group).[4−6] The NO fragment from the dissociation of *o*-nitrotoluene between 224 and 238 nm[7] and 220 and 250 nm[8] has also been observed.

Up to now, there has been no theoretical study on the decomposition of *o*-nitrotoluene, to our knowledge. In the present work, the kinetics and mechanism for the isomerization and decomposition of *o*-nitrotoluene have been computationally studied at the G2M(RCC, MP2) level of theory.[9] The potential energy surface (PES) and the rate constants for *o*-$CH_3C_6H_4NO_2 \rightarrow CH_3C_6H_4 + NO_2$, $C_6H_4C(H)ON$ (anthranil) + H_2O, $CH_3C_6H_4O$ + NO, and $CH_2C_6H_4NO$ + OH production channels have been predicted, and the results are reported herein for high-temperature combustion modeling applications.

Computational Method

The optimized geometries of *o*-nitrobenzene, its 8 stable isomers, 11 transition states, and products for the four dissociation channels have been calculated at the B3LYP/6-311G(d, p) level. To obtain more reliable values of energies for PES and rate constant predictions, we performed a series of single-point energy calculations for each molecule and transition state with the G2M(RCC, MP2) scheme[9] based on the optimized geometries at the B3LYP/6-311G(d, p) level. The G2M(RCC, MP2)//B3LYP method with larger basis sets is a reliable computational method for decomposition of phenyl compounds such as nitrobenzene[10] and nitrosobenzene.[11] The G2M(RCC, MP2) composite scheme is given as follows:

* Corresponding author. E-mail: chemmcl@emory.edu.
[†] National Chiao Tung University.
[‡] Emory University.

10.1021/jp0623591 CCC: $33.50
Published on Web 08/02/2006

$$E_0[\text{G2M}] = \text{RCCSD(T)/6-311G(d, p)} + \text{MP2/6-311+G(3df, 2p)} - \text{MP2/6-311G(d, p)} + \Delta\text{HLC} + \text{ZPE}$$

where the higher level corrections (ΔHLC) is given by $-5.3n_\beta - 0.19n_\alpha$ in millihartree, where n_α and n_β are the numbers of α and β valence electrons, respectively.

Results and Discussion

1. Isomerization and Dissociation of *o*-Nitrotoluene. The optimized structures of species **1**−**32** for *o*-nitrotoluene, its isomeric intermediates, transition states for the isomerization and dissociation reactions, and dissociated products calculated at the B3LYP/6-311G(d, p) level are presented in Figure 1. The energy diagram of the system, including various isomerization and decomposition reactions, computed with the G2M(RCC, MP2) method discussed above is shown in Figure 2. As shown in Figure 1, *o*-nitrotoluene has six different isomers: $CH_2C_6H_4$-*t*-N(OH)O (**6**), $CH_2C_6H_4$-*c*-N(OH)O (**8**), $CH_2C_6H_4N(O)OH$ (**10**), $C_6H_4C(H_2)ONOH$ (**13**), $CH_3C_6H_4ONO$ (**24**), and $CH_2(OH)C_6H_4$-NO (**27**); among them **27** is most stable, lying below the *o*-nitrotoluene at 4.1 kcal/mol. The geometries of *o*-nitrotoluene (**1**), **6**, **8**, and **10** have near C_s symmetry. Due to the ortho effect, the H atom of the $-CH_3$ group of *o*-nitrotoluene is transferred to the NO_2 group of the **6** by an isomerization reaction. The **6** is the conformer of the **8** due to the internal rotation of OH in the HONO group. The **8** isomerizes to the **10** by the H atom transfer (HONO ⇔ ONOH). The **8** isomerizes to the **27** by the OH group transfer from HONO to the CH_2 group. Isomerization reactions can occur among the isomers by their corresponding transition states. Similar to the nitro isomerization reaction of nitrobenzene,[10] *o*-nitrotoluene isomerizes to **24** by the nitro−nitrite isomerization reaction.

The *o*-nitrotoluene molecule can dissociate directly to the products $CH_3C_6H_4$ (**19**) + NO_2 with the dissociation energy at 0 K of 76.3 kcal/mol and to $C_6H_4NO_2$ (**18**) + CH_3 with the high dissociation energy at 0 K of 103.0 kcal/mol. The predicted C−NO_2 dissociation energy at 1100 K of 75.7 kcal/mol may be compared with the experimental activation energy measured at 1100 K and 110 Torr SF_6 pressure, 70.2 ± 2.5 kcal/mol.[1] $CH_3C_6H_4NO_2$ can also dissociate directly to give the products $C_6H_4CH_2$ (**4**) + HONO with a 63.6 kcal/mol enthalpy change after overcoming the 104.3 kcal/mol barrier at TS_1, and the products $C_6H_3CH_3$ (**22**) + HONO with the predicted enthalpy of reaction, 72.9 kcal/mol, after overcoming the 74.3 kcal/mol barrier at TS_8. In these reactions, species ONOH···$C_6H_4CH_2$ (**3**) and ONOH···$C_6H_3CH_3$ (**21**) appearing in the PES are product complexes. Isomer **13**, which can be formed by ring-closure from isomers $CH_2C_6H_4$-*c*-N(OH)O (**8**) and $CH_2C_6H_4N$-(O)OH (**10**) via TS_6 and TS_5, respectively, can eliminate H_2O to give the double-ring product $C_6H_4C(H)ON$ (**16**, anthranil) by overcoming the 37.7 kcal/mol barrier at TS_7 with −6.0 kcal/mol overall energy change from the reactant. Isomer $CH_3C_6H_4$-ONO (**24**), formed by the nitro−nitrite isomerization reaction from the reactant via TS_9 (57.9 kcal/mol), can dissociate readily to the products $CH_3C_6H_4O$ (**25**) + NO with an endothermicity of 14.3 kcal/mol or to the less favored products $CH_3C_6H_4$ (**19**) + NO_2 with an endothermicity of 76.3 kcal/mol as cited above for the direct dissociation process. Both dissociation reactions occur without intrinsic barriers. Isomer **8** and its isomer through HONO internal rotation, $CH_2C_6H_4$-*t*-N(OH)O (**6**)—the initial H-abstraction product from CH_3 by the nitro-group via TS_2 (46.3 kcal/mol)—can dissociate to produce $CH_2C_6H_4NO$ (**17**) + OH with 84.9 kcal/mol overall endothermicity and to $C_6H_4CH_2$ (**30**) + HONO with 92.2 kcal/mol endothermicity; both occur by direct dissociation mechanism. Finally, isomer *o*-hydroxymethyl nitrosobenzene (**27**), predicted to be the most stable isomer, can dissociate to give the products $CH_2(OH)C_6H_4$ (**28**) + NO and C_6H_4NO (**29**) + CH_2OH with 55.6 and 104.5 kcal/mol overall endothermicities, respectively, both by direct dissociation processes.

In summary, there are 10 decomposition channels for *o*-nitrotoluene and its isomers, where the channels giving rise to NO_2, H_2O, and NO products are major reactions. In addition, the OH loss process was also reported in some photodissociation experiments;[4−6] this process may involve the dissociation channels $CH_2C_6H_4N(O)OH$ (**10**) → $C_6H_4C(H_2)NO$ (**14**) + OH and $CH_2C_6H_4$-*t*-N(OH)O (**6**) or $CH_2C_6H_4$-*c*-N(OH)O (**8**) → $CH_2C_6H_4$-NO (**17**) + OH with 74.2 and 84.9 kcal/mol overall endothermicities, respectively; among them the first reaction with a much lower dissociation energy should dominate. Products **17** and **14** formed above are the two structural isomers of *o*-nitrosobenzyl radicals connected by the −NO torsional isomerization transition state.

2. Rate Constants Calculations.

a. Production of NO_2. The NO_2 elimination reaction

$$o\text{-}CH_3C_6H_4NO_2 \rightarrow C_6H_4CH_3 + NO_2 \qquad (1)$$

is a direct dissociation process, which is similar to $C_6H_5NO_2 \rightarrow C_6H_5 + NO_2$.[10] The predicted dissociation energy, 76.3 kcal/mol, is close to the analogous dissociation energy, 74.1 kcal/mol in $C_6H_5NO_2$. The rate constant for reaction 1, k_1, has been predicted with the Variflex code[12] based on the G2M(RCC) PES and the molecular parameters and frequencies computed by B3LYP/6-311G(d, p). For k_1 evaluation, the minimum energy path (MEP) representing the direct dissociation process was obtained by calculating the potential curve along the reaction coordinate C−N of o-$CH_3C_6H_4NO_2 \rightarrow CH_3C_6H_4 + NO_2$. Along the path, the C−N bond length was stretched from the equilibrium value 1.483 to 5 Å with the step size of 0.1 Å and each geometry with a fixed C−N bond length was fully optimized at the B3LYP/ 6-311G(d, p) level. The MEP with the separation of 2.3 to 5.0 Å in the variational TST calculation is approximated with the Morse potential, $V(r) = D_e[1 - \exp[-\beta(R - R_0)]]^2$, where R is the reaction coordinate, R_0 is the equilibrium value, and D_e is the bond energy without zero-point energy corrections. The parameters of the Morse potential obtained by fitting the MEP are $R_0 = 1.483$ Å, $\beta = 1.31$ Å^{-1}, and $D_e = 81.0$ kcal/mol, which was scaled slightly to the G2M value without ZPE-correction. The CH_3 groups in $CH_3C_6H_4$ and o-$CH_3C_6H_4NO_2$ were treated as free rotors with the rotational constants of 5.563 cm^{-1} for $CH_3C_6H_4$ and 5.415 cm^{-1} for o-$CH_3C_6H_4NO_2$ evaluated with the ChemRate program.[13] In addition, the Lennard-Jones pairwise potential and the anisotropic potential (a potential anisotropy form assuming a bonding potential which is cylindrically symmetric with respect to each fragment) are also added to form the final potential for the variational rate constant evaluation. To compare the theory with experiments, we have calculated the rate constants in the temperature range 500−2000 K under different experimental conditions. The Lennard-Jones (L-J) parameters for different bath gases employed are as follows: Ar, $\sigma = 3.47$ Å, $\epsilon/k = 114$ K;[14] SF_6, $\sigma = 5.20$ Å, $\epsilon/k = 212$ K;[14] o-$CH_3C_6H_4NO_2$, $\sigma = 5.6$ Å, $\epsilon/k = 690$ K, derived from its critical temperature (769 K) and volume (376 cm^3/mol) using the formulas ($\epsilon/k = 0.897\ T_c$, $\sigma = 0.785\ V_c^{1/3}$).[14] The average step-sizes for collisional deactivation by Ar and SF_6 were taken as $\langle\Delta E\rangle_{down} = 400$ and 2200 cm^{-1}, respectively, as previously employed for the $C_6H_5NO_2$ decomposition reaction.[10]

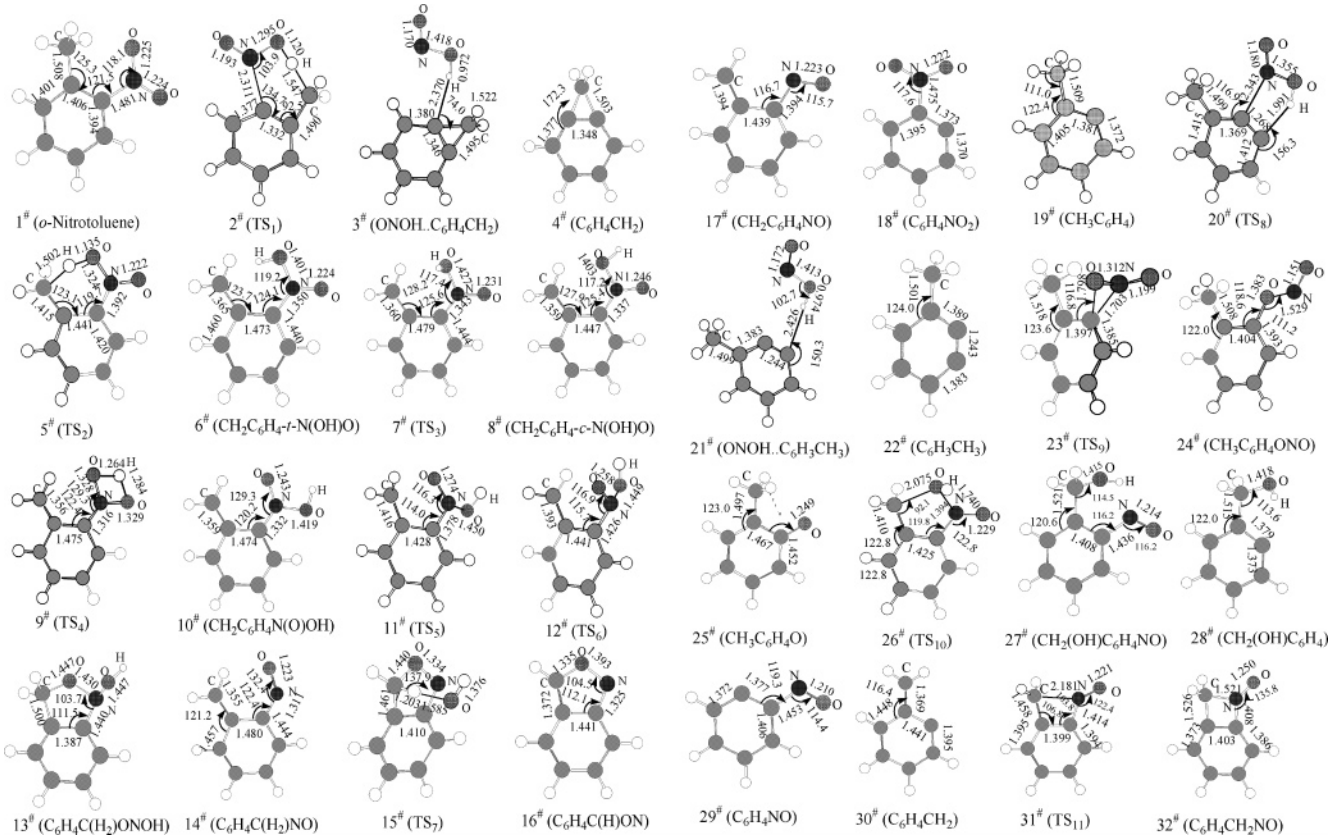

Figure 1. Optimized geometries of *o*-nitrotoluene, its isomers, transition states for the isomerization and dissociation reactions, and dissociation products calculated at the B3LYP/6-311G(d, p) level.

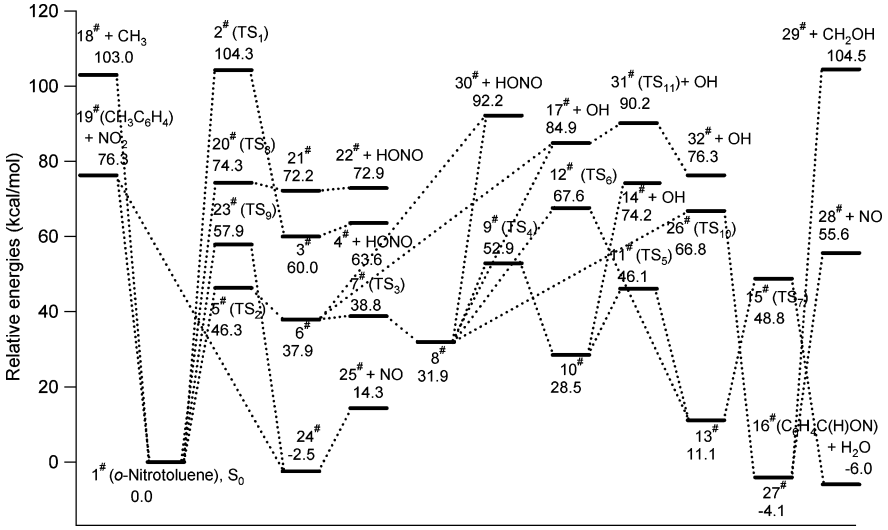

Figure 2. Schematic energy diagram for decomposition and dissociation reactions of *o*-nitrotoluene calculated at the G2M(RCC, MP2)//B3LYP/6-311G(d, p) level, where energy is given in kcal/mol.

The predicted high-pressure first-order and low-pressure second-order rate constants for the decomposition reaction in the temperature range 500−2000 K can be represented by

$$k_{1\infty} = 4.10 \times 10^{17} \exp[-37000/T]\ \mathrm{s}^{-1},$$

$$k_1^{\,0} = 5.41 \times 10^{101} \times T^{-24.3} \exp[-43500/T]\ \mathrm{cm}^3\,\mathrm{mol}^{-1}\,\mathrm{s}^{-1}$$

for the Ar-bath gas. The high value of the high-pressure *A*-factor given above is consistent with those obtained for C_6H_5NO[11] and $C_6H_5NO_2$[10] fragmentation reactions.

The predicted values shown in Figure 3 for the conditions close to those employed experimentally compare reasonably with the experimental results cited in the Introduction. The rate constants measured by Gonzalez et al.[1] using the SF_6 as bath gas at 110 Torr pressure are evidently higher than those measured by Tsang and co-workers[2,3] using Ar as bath gas at 2700−3400 Torr. The values predicted for the conditions employed by Gonzalez et al.[1], represented by $k_1 = 1.5 \times 10^{15} \exp[-30900/T]\ \mathrm{s}^{-1}$, though slightly lower than their experimental results given by $k_1 = 7.9 \times 10^{15} \exp[-(33000 \pm 1000)/T]\ \mathrm{s}^{-1}$, are well within the given error bars as shown in the

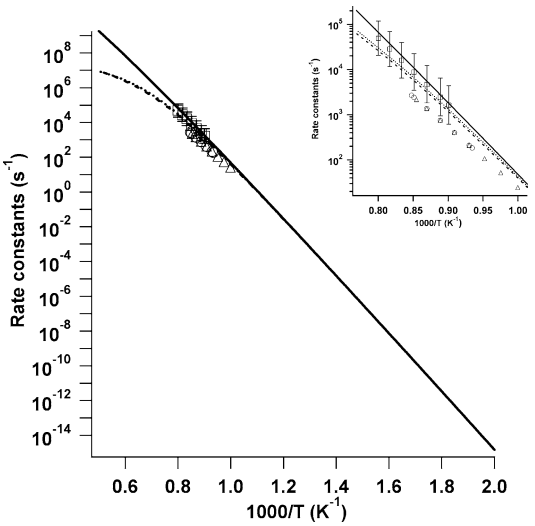

Figure 3. Predicted rate constants for NO_2 production. Experimental data: ○, ref 2; □, ref 1; △, ref 3. Predicted values: solid line, the high-pressure limit; dotted curve, rate constants with Ar as bath gas at 3000 Torr; dashed curve, rate constants with 110 Torr SF_6 in the temperature range of 500−2000 K.

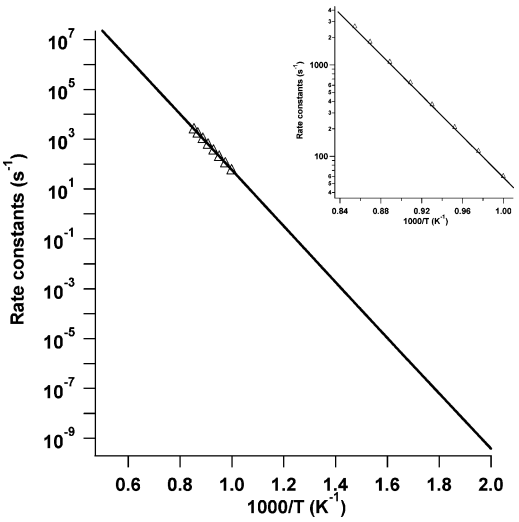

Figure 4. Predicted rate constants for anthranil formation. Experimental data: △, ref 3. Predicted values: solid line, rate constants with Ar as bath gas at 3000 Torr in the temperature range of 500−2000 K.

figure. However, the rate constants predicted for the conditions employed by Tsang and co-workers,[2,3] represented by $k_1 = 1.6 \times 10^{16} \exp[-33500/T]\ s^{-1}$, are noticeably higher than their experimental values given by $k_1 = 6.4 \times 10^{14} \exp[-30900/T]\ s^{-1}$. In both experiments cited above, internal kinetic standards were employed; Gonzalez et al. used cyclohexene[1] while Tsang and co-workers[2] employed 1,2-dimethyl cyclohexene. Tsang and co-workers[2] also mentioned that the rate constants of *o*-nitrotoluene decomposition obtained by Gonzalez et al.[1] were approximately a factor of 3 higher than the data they obtained. It should be noted that for the decomposition of nitrobenzene our predicted rate constants for NO_2 production[10] were found to agree closely with the results of both Gonzalez et al. in ref 1 and Tsang et al. reported in ref 2 under their conditions employed.

b. Production of Anthranil by Dehydration. The dehydration reaction

$$o\text{-}CH_3C_6H_4NO_2 \rightarrow C_6H_4C(H)ON + H_2O \qquad (2)$$

is a complex isomerization/decomposition process; it can take place by the following two paths:

$$o\text{-}CH_3C_6H_4NO_2 \overset{TS_2}{\longleftrightarrow} CH_2C_6H_4\text{-}t\text{-}N(OH)O\ (\mathbf{6}) \overset{TS_3}{\longleftrightarrow}$$
$$CH_2C_6H_4\text{-}c\text{-}N(OH)O\ (\mathbf{8}) \overset{TS_4}{\longleftrightarrow} CH_2C_6H_4N(O)OH\ (\mathbf{10}) \overset{TS_5}{\longleftrightarrow}$$
$$C_6H_4C(H_2)ONOH\ (\mathbf{13}) \overset{TS_7}{\longrightarrow} C_6H_4C(H)ON + H_2O \quad (2a)$$

$$o\text{-}CH_3C_6H_4NO_2 \overset{TS_2}{\longleftrightarrow} CH_2C_6H_4\text{-}t\text{-}OHNO\ (\mathbf{6}) \overset{TS_3}{\longleftrightarrow}$$
$$CH_2C_6H_4\text{-}c\text{-}OHNO\ (\mathbf{8}) \overset{TS_6}{\longleftrightarrow}$$
$$C_6H_4C(H_2)ONOH\ (\mathbf{13}) \overset{TS_7}{\longrightarrow} C_6H_4C(H)ON + H_2O \quad (2b)$$

In reactions 2a and 2b, the geometries and energies for the reactant, intermediates, transition states, and products are shown in Figures 1 and 2, respectively. In reaction 2a, the transition state TS_4 with a 52.9 kcal/mol barrier is the primary rate-controlling step while in reaction 2b, TS_6 with a 67.6 kcal/mol barrier controls the rate of the reaction by this path. The predicted rate constants for these multiple-well decomposition processes in the temperature range 500−2000 K computed with the ChemRate program[13] were found to be weakly pressure-dependent. The values predicted at 3000 Torr pressure with Ar as bath gas can be represented by the expressions

$$k_{2a} = 8.79 \times 10^{12} \exp[-25800/T]\ s^{-1},$$

$$k_{2b} = 3.65 \times 10^{13} \exp[-34700/T]\ s^{-1}.$$

The total rate constant, $k_2 = k_{2a} + k_{2b}$, can be represented by the expression

$$k_2 = 9.09 \times 10^{12} \exp[-25800/T]\ s^{-1}$$

to which k_{2b} is predicted to contribute only 1−2% over the wide range of temperature studied. The rate expression predicted for the atmospheric pressure is essentially the same with $k_2 = 8.96 \times 10^{12} \exp[-25800/T)\ s^{-1}$.

As shown in Figure 4, the predicted values of k_2 given by $9.8 \times 10^{12} \exp[-25900/T]\ s^{-1}$ in the experimental temperature range 1100−1170 K are in excellent agreement with the experimental data,[3] $k_2 = 1.2 \times 10^{13} \exp[-26000/T]\ s^{-1}$.

c. Production of NO. As shown in Figure 2, this decomposition process can take place via TS_9 and **24**:

$$o\text{-}CH_3C_6H_4NO_2 \overset{TS_9}{\longleftrightarrow} \mathbf{24} \rightarrow CH_3C_6H_4O + NO \qquad (3)$$

A similar nitro−nitrite isomerization/decomposition process has been studied in the nitrobenzene decomposition reaction.[10] Because the barrier at TS_9 is 43.6 kcal/mol higher than the dissociation energy of $CH_3C_6H_4ONO$ (**24**) → $CH_3C_6H_4O$ (**25**) + NO with 14.3 kcal/mol, this decomposition reaction can be treated as a one-step dissociation via TS_9. The predicted barrier, 57.9 kcal/mol, may be compared with that of the parallel nitrobenzene decomposition reaction, 61.1 kcal/mol. The statistical factor for the decomposition reaction is 2 because there are two optical isomers in TS_9.

The predicted rate constant for reaction 3 in the temperature range 500−2000 K calculated by the Variflex code[12] for the high-pressure first-order and low-pressure second-order limits

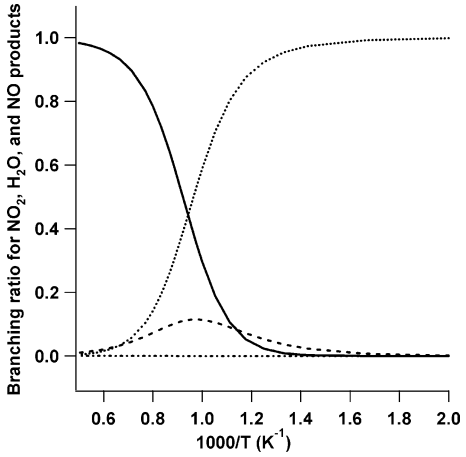

Figure 5. Calculated branching ratios for the four channels of *o*-nitrotoluene decomposition to NO_2 (solid curve), H_2O (dotted curve), NO (dashed curve), and OH (dash−dotted curve) products in the temperature range 500−2000 K.

in Ar can be represented by the expressions,

$$k_3^{\infty} = 1.49 \times 10^{14} \exp[-30000/T]\ \mathrm{s}^{-1},$$

$$k_3^{0} = 6.21 \times 10^{92} \times T^{-21.8} \exp[-36000/T]\ \mathrm{cm}^3\,\mathrm{mol}^{-1}\,\mathrm{s}^{-1}.$$

To our knowledge, there are no experimental rate constants available for the decomposition channel of NO product.

d. Production of OH. As mentioned in the last section,

$$CH_2C_6H_4N(O)OH\ (\mathbf{10}) \rightarrow CH_2C_6H_4NO\ (\mathbf{14}) + OH \quad (4)$$

with 74.2 kcal/mol dissociation energy is the primary channel of the OH product. The isomerization process from *o*-$CH_3C_6H_4NO_2$ to $CH_2C_6H_4N(O)OH$ (**10**) is the same as reaction 2.

The predicted rate constant for reaction 4 in the temperature range 500−2000 K calculated by the ChemRate program[13] for the high-pressure first-order and low-pressure second-order limits in Ar can be represented by the expressions

$$k_4^{\infty} = 1.31 \times 10^{13} \exp[-39000/T]\ \mathrm{s}^{-1},$$

$$k_4^{0} = 2.67 \times 10^{28} \times T^{-3.7} \exp[-34000/T]\ \mathrm{cm}^3\,\mathrm{mol}^{-1}\,\mathrm{s}^{-1}.$$

To our knowledge, there are no experimental data available for the decomposition channel producing the OH product.

e. The Branching Ratios for Formation of NO_2, H_2O, NO, and OH. The branching ratios of high-pressure rate constants for *o*-nitrotoluene to produce NO_2, H_2O, NO, and OH are shown in Figure 5. The channel for H_2O production dominates at temperatures below 1000 K, whereas that for NO_2 production becomes predominant over 1100 K. The channel producing NO accounts for only 5−10% of the total decomposition rates in the temperature range from 800 to 1300 K. The channel producing OH contributes negligibly to the total decomposition rate.

Conclusions

The potential energy surface for the isomerization and decomposition of *o*-nitrotoluene, a model compound for TNT, has been calculated at the G2M(RCC, MP2)//B3LYP/6-311G-(d, p) level. There are 10 decomposition channels for *o*-nitrotoluene and its six isomeric derivatives, where the channels producing $CH_3C_6H_4 + NO_2$, $C_6H_4C(H)ON$ (anthranil) + H_2O, and $CH_3C_6H_4O$ (*o*-methyl phenoxy) + NO are primary processes. The predicted rate constants for NO_2 elimination (k_1) and for anthranil formation (k_2) are generally in reasonable agreement with available experimental data. The predicted rate constants for production of NO and OH (giving $CH_2C_6H_4NO$) were found to be much smaller. The branching ratios for *o*-nitrotoluene decomposition to produce NO_2, H_2O, NO, and OH in the temperature range 500−2000 K indicate that the dehydration process dominates at temperatures below 1000 K, whereas the NO_2 elimination reaction becomes dominant at temperature over 1100 K; and the NO product accounts for only 5−10% of the total yield in the temperature range from 800 to 1300 K. The channel producing OH is negligible over the entire range of temperature studied.

Acknowledgment. S.C.X. is grateful for the support of the Emerson Center for Scientific Computations at Emory University for an Emerson Visiting Fellowship. M.C.L. acknowledges the support from the Taiwan Semiconductor Manufacturing Company for the TSMC Distinguished Professorship and for the National Science Council of Taiwan for the Distinguished Visiting Professorship at National Chiao Tung University in Hsichu, Taiwan.

Supporting Information Available: Table S1 lists the frequencies and moments of inertia I_i of the decomposition reaction of *o*-nitrotoluene calculated at the B3LYP/6-311G(d, p) level. Table S2 lists the predicted forward and reverse rate constants of each and final rate constants of reaction 1, 2a, 2b, 3, and 4 at the high-pressure limit condition. This material is available free of charge via the Internet at http://pubs.acs.org.

References and Notes

(1) Gonzalez, A. C.; Larson, C. W.; McMillen, D. F.; Golden, D. M. *J. Phys. Chem.* **1985**, *89*, 4809.
(2) Tsang, W.; Robaugh, D.; Mallard, W. G. *J. Phys. Chem.* **1986**, *90*, 5968.
(3) He, Y. Z.; Cui, J. P.; Mallard, W. G.; Tsang, W. *J. Am. Chem. Soc.* **1988**, *110*, 3754.
(4) Kosmidis, C.; Ledingham, K. W. D.; Kilic, H. S.; McCanny, T.; Singhal, R. P.; Langley, A. J.; Shaikh, W. *J. Phys. Chem. A* **1997**, *101*, 2264.
(5) Shao, J.; Baer, T. *Int. J. Mass Spectrom. Ion Processes* **1988**, *86*, 357.
(6) McLuckey, S. A.; Glish, G. L. *Org. Mass Spectrom.* **1987**, *22*, 224.
(7) Marshall, A.; Clark, A.; Ledingham, K. W. D.; Sander, J.; Singhal, R. P. *Int. J. Mass Spectrom. Ion Processes* **1993**, *125*, R21.
(8) Castle, K. J.; Abbott, J. E.; Peng, X.; Kong, W. *J. Phys. Chem. A* **2000**, *104*, 10419.
(9) Mebel, A. M.; Morokuma, K.; Lin, M. C. *J. Chem. Phys.* **1995**, *103*, 7414.
(10) Xu, S. C.; Lin, M. C. *J. Phys. Chem. B* **2005**, *109*, 8367.
(11) Tzeng, C. M.; Choi, Y. M.; Huang, C. L.; Ni, C. K.; Lee, Y. T.; Lin, M. C. *J. Phys. Chem. A* **2004**, *108*, 7928.
(12) Klippenstein, S. J.; Wagner, A. F.; Dunbar, R. C.; Wardlaw, D. M.; Robertson, S. H. *Variflex* **1999**.
(13) Mokrushin, W.; Bedanov, V.; Tsang, W.; Zachariah, M.; Knyazev, V. *ChemRate*, Version 1.20; National Institute of Standards and Technology: Gaithersburg, MD 20899, 2003.
(14) Mourits, F. M.; Rummens, F. H. A. *Can. J. Chem.* **1977**, *55*, 3007.